

THE BINARY NUCLEUS IN VCC 128: A CANDIDATE SUPERMASSIVE BLACK HOLE IN A DWARF ELLIPTICAL GALAXY

VICTOR P. DEBATTISTA,^{1,2} IGNACIO FERRERAS,³ ANNA PASQUALI,⁴ ANIL SETH,^{1,5} SVEN DE RIJCKE,⁶ AND LORENZO MORELLI⁷

Received 2006 August 9; accepted 2006 September 29; published 2006 October 26

ABSTRACT

Hubble Space Telescope (HST) Wide Field Planetary Camera 2 (WFPC2) images of the Virgo Cluster dwarf elliptical galaxy VCC 128 reveal an apparently double nucleus. The two components, which are separated by ~ 32 pc in projection, have the same magnitude and color. We present a spectrum of this double nucleus and show that it is inconsistent with one or both components being emission-line background objects or foreground stars. The most likely interpretation is that, as suggested by Lauer et al. for the double nucleus in NGC 4486B, we are seeing a nuclear disk surrounding a supermassive black hole. This is only the second time an early-type dwarf (dE/dSph) galaxy has been suggested to host a supermassive black hole.

Subject headings: galaxies: dwarf — galaxies: individual (VCC 128) — galaxies: nuclei — galaxies: photometry — galaxies: stellar content

Online material: color figures

1. INTRODUCTION

The centers of galaxies often host supermassive black holes (SMBHs) with masses M_\bullet ranging from $\sim 10^6$ to $\sim 10^9 M_\odot$ (Kormendy & Richstone 1995). SMBH masses exhibit a variety of scaling relations including the M_\bullet - σ relation (Gebhardt et al. 2000; Ferrarese & Merritt 2000) and an M_\bullet - M_{DM} relation, where M_{DM} is the mass of the host dark matter halo (Ferrarese 2002; Baes et al. 2003). These correlations are evidence of a coupling between the formation of SMBHs and the formation of galaxies. One key to unraveling this coupling is to identify the seeds of SMBHs in dwarf galaxies. Ground-based stellar kinematic data of dwarf elliptical (dE) galaxies (Geha et al. 2002) rule out $M_\bullet \geq 10^7 M_\odot$. In the M31 globular cluster G1, thought to be the stripped nucleus of an accreted dE galaxy, Gebhardt et al. (2002) report finding an intermediate-mass black hole (IMBH) with $M_\bullet \sim 10^4 M_\odot$, consistent with the extrapolation of the M_\bullet - σ relation. Nuclear activity in low-luminosity dwarf galaxies has turned up a number of IMBHs with estimated masses from 10^4 to $10^6 M_\odot$ (Filippenko & Ho 2003; Barth et al. 2004; Greene & Ho 2004). There is no evidence of a SMBH in either M33 (Merritt et al. 2001; Gebhardt et al. 2001) or NGC 205 (Valluri et al. 2005). The paucity of SMBHs in dwarf galaxies led Ferrarese (2002) to suggest that low-mass galaxies are inefficient at forming SMBHs. Côté et al. (2006), Ferrarese et al. (2006), and Wehner & Harris (2006) find instead a continuity in scaling relations, with M_\bullet replaced by M_{CMO} , the mass of a central massive object, which is either a SMBH or a compact nucleus.

HST does not permit many dynamical M_\bullet measurements below $\sim 10^6 M_\odot$. An alternative approach to finding SMBHs in

low surface brightness dwarf galaxies is a morphological one. In a few galaxies, *HST* has found double nuclei; the clearest examples are in M31 and in NGC 4486B (Lauer et al. 1993, 1996, 2005). The two nuclei in M31, dubbed P1 and P2, are separated by 0.49 or 3.6 pc and have unequal surface brightness, with P2 having the lower surface brightness but sitting very close to the global photocenter. In contrast, in NGC 4486B the two nuclei are equal in magnitude, color, and displacement from the photocenter, with a total separation of 12 pc. The generally accepted model of the nucleus in M31 identifies P2 as the center of the galaxy surrounding its SMBH and P1 as the bright off-center apapsis of an eccentric Keplerian disk (Tremaine 1995). Self-consistent models and simulations of such nuclei can be constructed (Salow & Statler 2001; Jacobs & Sellwood 2001; Sambhus & Sridhar 2002). Lauer et al. (1996) proposed a similar model for the double nucleus in NGC 4486B, with the difference that the SMBH is located on the global photocenter between the two peaks. They suggested that binary nuclei are morphological indicators of SMBHs.

Here we present another example of a galaxy with a double nucleus, the Virgo Cluster dE galaxy VCC 128. Its nucleus is very similar to that of NGC 4486B. In § 2 we present the archival *HST* data, in § 3 we present new spectra and their modeling, and in § 4 we propose that the double nucleus is best explained by a disk surrounding a SMBH at the center of VCC 128 and explore its likely position in the M_\bullet - σ plane.

2. ANALYSIS OF *HST* ARCHIVAL IMAGES

Using the *HST* archive, we explored the nuclear morphologies of the sample of dE galaxies imaged in the WFPC2 snapshot surveys, proposals GO-8600 and GO-6352 (PI: H. Ferguson). These surveys imaged 50 galaxies, which were analyzed by Lotz et al. (2004) to show that typical dE stellar envelopes are 0.1–0.2 mag redder in $V - I$ than their nuclei. In most of the galaxies we either found no nucleus or a single nucleus. VCC 1107, FCC 208, and VCC 128 contained what appeared to be double nuclei; of these the two nuclei in VCC 128 are the closest and are most similar in magnitudes, making this galaxy a prime candidate for spectroscopic follow-up.

VCC 128 (UGCA 275) is a dE galaxy of $m_B = 15.6$ ($M_B = -15.5$) on the outskirts of the Virgo Cluster. VCC 128

¹ Astronomy Department, University of Washington, Box 351580, Seattle WA 98195; debattis@astro.washington.edu.

² Brooks Prize Fellow.

³ Physics Department, King's College London, Strand, London WC2R 2LS, UK; ferreras@star.ucl.ac.uk.

⁴ Max-Planck-Institut für Astronomie, Königstuhl 17, D-69117 Heidelberg, Germany; pasquali@mpia-hd.mpg.de.

⁵ Currently a CfA Postdoctoral Fellow, 60 Garden Street, Cambridge, MA 02138; aseth@cfa.harvard.edu.

⁶ Sterrenkundig Observatorium, Universiteit Gent, Krijgslaan 281, S9, B-9000 Gent, Belgium; Sven.DeRijcke@UGent.be.

⁷ Departamento de Astronomía y Astrofísica, Pontificia Universidad Católica de Chile, Casilla 306, Santiago 22, Chile; lmorelli@astro.puc.cl.

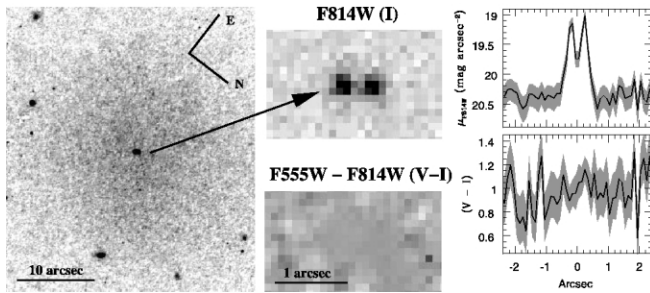


FIG. 1.—WFPC2 F814W image of VCC 128 (*left panel*, $32'' \times 37''$). In the top middle panel, we zoom into the central $2.5'' \times 1.5''$, showing that the nucleus is resolved into two components. P1 is the nucleus to the southwest (*left*), and P2 is the one to the northeast (*right*). The nuclei are located at R.A. = $12^{\text{h}}14^{\text{m}}59^{\text{s}}.71$, decl. = $09^{\circ}33'55''.57$ (P1) and R.A. = $12^{\text{h}}14^{\text{m}}59^{\text{s}}.73$, decl. = $09^{\circ}33'55''.82$ (P2) in J2000.0 coordinates. The bottom middle panel shows the same zoom into the $V-I$ color map, where $(V-I)$ ranges between 1 and 2 mag, reaching ~ 1.0 in the double nucleus. The top right panel shows the light profile of a slit 5 pixels across along the major axis of the nucleus. The shaded region indicates $\pm 1\sigma$ error. The bottom right panel shows the color profile for the same slit. [See the electronic edition of the *Journal* for a color version of this figure.]

was imaged for 460 s in the F555W (V -band) filter and 300 s in the F814W (I -band) filter. Its two nuclei are separated by 4 WF3 pixels (see Fig. 1), i.e., ~ 0.4 or 32 pc (assuming a Virgo Cluster distance of 16.5 Mpc; Tonry et al. 2001; Jerjen et al. 2004). We label the component to the southwest as P1 and the one to the northeast as P2. These are equally bright, with apparent magnitudes $\approx 22.56 \pm 0.05$ ($M_V = -8.5$ in P1) and $\approx 22.72 \pm 0.06$ (P2) in the F555W filter and $V-I = 0.9 \pm 0.07$ (P1) and 1.15 ± 0.07 (P2). The signal-to-noise ratio (S/N) is 4.3–5.0 in V and 6.2–6.6 in I for the two nuclei measured with an aperture of radius 2 pixels. The $V-I$ color map (Fig. 1) shows that the double nucleus is not caused by patchy obscuration. Each nucleus is resolved, with FWHMs (from a Gaussian fit) of 3.1 and 3.9 pixels in the I band, whereas the filter point-spread function FWHM is 1.3 pixels.

The surface brightness profile of VCC 128 is quite flat, and ellipse fitting in IRAF is unstable. Using GALFIT (Peng et al. 2002), we fitted the surface brightness using a Sérsic model, after masking out stars and the nuclei. We obtained a Sérsic index $n = 0.35$ and a half-light radius $R_{\text{eff}} = 9''$ for F814W, and $n = 0.55$ and $R_{\text{eff}} = 14.5''$ for F555W. The circumnuclear region (measured within $1''$ of the nuclei) has a surface brightness $\mu_V = 21.37 \pm 0.07$ and color $\mu_V - \mu_I \approx 1.0 \pm 0.1$. The average surface brightness within R_{eff} (averaged between V and I bands) is $\mu_V = 23.95 \pm 0.02$ mag arcsec $^{-2}$ and $\mu_I = 22.94 \pm 0.02$ mag arcsec $^{-2}$. The midpoint between the centroids of the two nuclei (measured within an aperture of 2 pixels) is offset by $\sim 0.8''$ (~ 60 pc) from the photocenter of the galaxy as fitted by GALFIT, but with these shallow images we cannot determine whether the photocenter varies with radius as in other offset nuclei (De Rijcke & Debattista 2004). Possibly because of this offset, Lotz et al. (2004) classified VCC 128 as nonnucleated.

3. SPECTRAL ENERGY DISTRIBUTION

3.1. Observations and Reductions

We obtained long-slit spectra through the nucleus of VCC 128 at the Apache Point Observatory 3.5 m telescope using the Double Imaging Spectrograph with $0.4''$ pixels. We used the blue grating with a low resolution of $2.4 \text{ \AA pixel}^{-1}$ over the

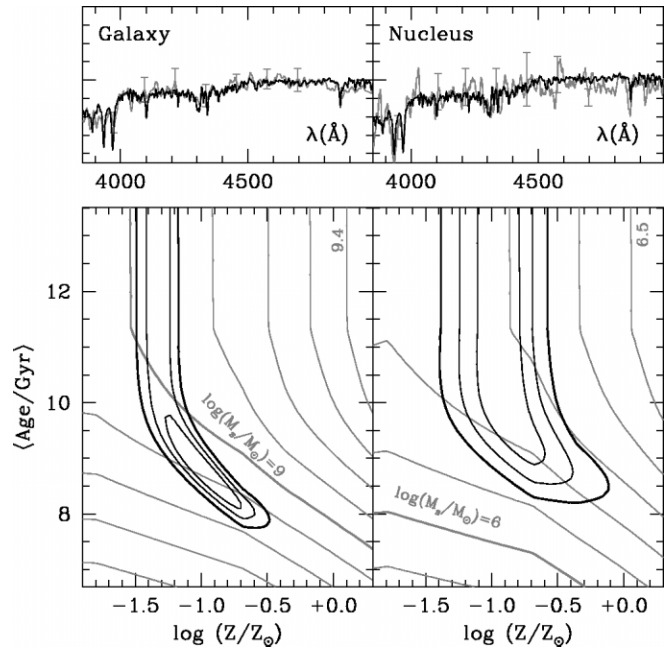


FIG. 2.—*Top*: Observed (smoothed) SEDs. The two panels compare the SED of the galaxy (*left*) and the nucleus (*right*) (*gray line*) with the best-fitting model SED (*black lines*). The feature at $\sim 4800 \text{ \AA}$ in the observed spectra is due to an artifact of the flux calibration due to a “bump” in the grating response, while that at $\sim 4600 \text{ \AA}$ in the nuclear spectrum is a remnant of the background subtraction. *Bottom*: Corresponding mean properties of the best-fitting stellar populations. Confidence levels (*black lines*) are given at the 1, 2, and 3σ (*thick lines*) levels. Contours of stellar mass are shown in both cases (*gray lines*). For the nucleus, the mass shown is for the two components combined.

wavelength range $3660 \text{ \AA} \leq \lambda \leq 5600 \text{ \AA}$. The data were obtained during two runs. In the first run on 2005 March 8, we obtained a total of 5.3 hr of data using a $1.5''$ slit. Seeing conditions varied significantly over the night, ranging from $0.8''$ to $>2''$, and we had difficulty pointing at the nucleus during some of the exposures. Unsurprisingly, the double nucleus can be detected only in two 1 hr exposures from this run. Therefore, we also obtained data during a second run on 2006 April 21 under subarcsecond seeing. During this run we used the $0.9''$ slit to obtain two 1 hr spectra.

The spectra were reduced with IRAF using standard tasks. Flux calibration, using the standard stars BD 18 2647 for the first run and BD 26 2606, Feige 98, and HR 4554 for the second run, achieved a 7% uncertainty at wavelengths bluer than 4000 \AA , increasing to 10% at 5500 \AA . Data from the two runs were combined by smoothing the 2006 data to match the FWHM of the 2005 run (6 \AA , or 454 km s^{-1} at the Ca II lines). The spectrum of the nucleus (spatially unresolved from the ground) is typically 6 pixels wide along the cross-dispersed axis, and that of the galaxy 51 pixels. We extracted the spectrum of the nucleus from the four exposures, integrated over the 6 central pixels. The galaxy’s spectrum was extracted below and above the nucleus for a total extension of 45 pixels along the spatial direction. To remove the galaxy contamination in the spectrum of the nucleus, we subtracted the scaled galaxy spectrum from it. The individual spectra of the nucleus and the galaxy were then averaged to increase their S/N, which turned out to be ~ 2 and $\sim 8 \text{ pixel}^{-1}$, respectively. The spectra of the galaxy and of the nucleus are shown in Figure 2. At the nucleus, $\sim 12\%$ of the light comes from the nuclei, the rest being due to the galaxy.

3.2. Spectral Analysis

The absence of emission lines in the nuclear spectrum rules out, at high confidence, that either P1 or P2 is a background emission-line object. A foreground star can be ruled out on several counts. The nuclei are both resolved by *HST*, and standard models of the Milky Way (Bahcall & Soneira 1980) predict only 0.22 stars of this magnitude to fall within $2R_{\text{eff},V} = 29''$ in this part of the sky. We also used our spectra to measure the velocities of the galaxy and of the nuclei from the centroid of a Gaussian fit to the Ca II H and K lines. For the galaxy we obtained $v = 1331 \pm 184 \text{ km s}^{-1}$, and for the nuclei $1179 \pm 185 \text{ km s}^{-1}$ (heliocentric). As these lines have very low S/N, we also measured velocities by modeling the entire spectral energy distribution (SED) assuming various stellar templates from the Pickles (1998) library. We considered templates of solar metallicity, although fits to nonsolar metallicities will not change the outcome of the analysis. Figure 3 shows the reduced χ^2 for 704 degrees of freedom of a comparison in the spectral range $3880 \text{ \AA} \leq \lambda \leq 5000 \text{ \AA}$, which includes the 4000 \AA break, the G-band step, Balmer features, and metallic absorption lines. Wavelengths outside this range have very low S/N. Galactic reddening was applied using the prescription [$R = A_V/E(B - V) = 3.1$] of Fitzpatrick (1999) for a color excess of $E(B - V) = 0.015$ (Schlegel et al. 1998). The filled circles in Figure 3 span the temperature range from O5 (right) to M6 for dwarfs (black lines) and from O8 to M9 for giants (gray line). The $\tilde{\chi}^2$ is shown as a function of distance, which is computed by comparing the apparent and absolute magnitudes corresponding to each star. Overall, the best-fitting foreground star would be a G8 V dwarf at 25 kpc ($\tilde{\chi}^2 = 1.23$) with $v = 1190^{+289}_{-190} \text{ km s}^{-1}$. All fits with $\tilde{\chi}^2 < 2$ require $v > 500 \text{ km s}^{-1}$, which is improbable for stars in the Milky Way halo. Hence, neither source at the center of VCC 128 can be a foreground star, but they are in good agreement with Virgo Cluster membership, leading us to conclude that this is the nucleus of VCC 128.

To estimate the mass of the nucleus, we compared the SEDs of both the galaxy and the nucleus with the population synthesis models of Bruzual & Charlot (2003). We generated a 64×64 grid of τ -models, i.e., composite stellar populations according to an exponentially decaying star formation rate that are then modeled at the resolution and pixel sampling of the observations, and compared via a maximum likelihood analysis. The formation epoch was fixed at $z_F = 3$. The two parameters explored in the grid are the exponential star formation timescale [$-1 < \log(\tau/\text{Gyr}) < 1$] and the metallicity [$-2 < \log(Z/Z_\odot) < +0.3$]. Figure 2 shows the 1, 2, and 3 σ (thick lines) confidence levels for the analysis of the galaxy (left) and of the nucleus (right). The plots overlay contours of stellar mass corresponding to the observed apparent magnitude assuming a Chabrier (2003) initial mass function (IMF), and using the total apparent magnitude of the galaxy ($m_B = 15.6$; Binggeli et al. 1985) and of the double nucleus combined. Our results for the ages and metallicities are independent of the assumed IMF, but the masses are more sensitive to this change. The nucleus is consistent with having a relatively metal-rich stellar population older than 8 Gyr. With the assumed IMF, the best-fit combined nuclear stellar mass is $\sim 10^6 M_\odot$. The galaxy spectrum gives—within error bars—a similar value for the age and metallicity.

In order to assess the effect of dust on the SED analysis, we ran a few sets of grids for various values of $E(B - V)$. The

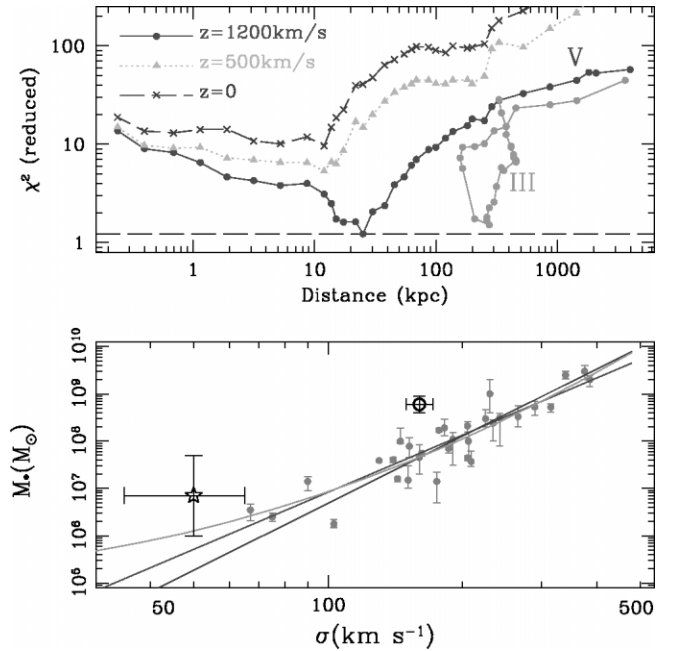


FIG. 3.—*Top*: Analysis of the nuclear spectrum assuming it is a star. The black lines compare the observed SED with a range of dwarf stars (O–M). The gray line corresponds to a range of giant stars. We use $V = 22.6$ to derive distances. The dashed and dotted lines correspond to an assumed velocity = 0 and 500 km s⁻¹, respectively, whereas the solid lines are computed for the best estimate— $v = 1190^{+289}_{-190} \text{ km s}^{-1}$ at 95% confidence level—computed by cross-correlating the observed SED with the stellar template that gives the best fit (G8 V, $M_V = +5.6$). The best fit for a giant is a G5 III ($M_V = +0.4$) with $\tilde{\chi}^2 = 1.52$. *Bottom*: Estimated location of VCC 128 (open star) on the M_\bullet - σ plane. The solid circles are the compilation of Tremaine et al. (2002), with the solid line showing their best-fit relation. The dashed and dotted lines show the relation as derived by Merritt & Ferrarese (2001) and Wyithe (2006), respectively. The open circle shows NGC 4486B from Kormendy & Gebhardt (2001) and J. Kormendy (2006, private communication). [See the electronic edition of the Journal for a color version of this figure.]

best fits obtained for these realizations gave consistently higher values of χ^2 , so that a color excess above $E(B - V) > 0.1 \text{ mag}$ is ruled out at the 3σ level.

4. DISCUSSION AND CONCLUSIONS

Since the nucleus is old, the present configuration could not have resulted from recent gas infall. It is unlikely, though not impossible, that the two nuclei are both globular clusters 32 pc apart in the last stages of merging because of the short lifetime of such a configuration ($\sim 5 \text{ Myr}$ using the standard Chandrasekhar 1943 formula with $\ln \Lambda = 4$ and $v_c = 20 \text{ km s}^{-1}$). Two well-separated globular clusters projected so close to each other, so close to the center of the galaxy, and so similar in their properties are even more unlikely. The double nucleus in VCC 128 is similar in many ways to that in NGC 4486B. As in NGC 4486B, a nuclear disk surrounding a SMBH provides the best explanation: this would be a stable, long-lived configuration, and would account for the similar colors and magnitudes of the two components and for their location near the center of the galaxy.

If the double nucleus is a disk orbiting a SMBH, we can estimate a lower limit to M_\bullet by assuming that it is larger than the nuclear disk mass, $M_d = 10^6 M_\odot$. Alternatively, we can use the ratio of M_d to M_\bullet in M31 ($M_d/M_\bullet = 0.16$; Tremaine 1995) and in NGC 4486B ($M_d/M_\bullet = 0.019$; Kormendy et al. 1997; Lauer et al. 1996) to estimate $M_\bullet \sim 6 \times 10^6 - 5 \times 10^7 M_\odot$ in VCC 128. We estimate a velocity dispersion, σ , for VCC 128

from the Faber-Jackson relation of dE galaxies (de Rijcke et al. 2005). We obtain $\sigma \sim 35\text{--}65 \text{ km s}^{-1}$. Thus, within large uncertainties, the postulated SMBH in VCC 128 could satisfy the M_{\bullet} - σ relation, as we show in Figure 3.

Ferrarese (2002) proposed that galaxies with a dark matter virial velocity $v_{\text{vir}} \lesssim 200 \text{ km s}^{-1}$ would not be able to form SMBHs. Using her scaling relations between σ and v_{vir} , we find that $v_{\text{vir}} \lesssim 65 \text{ km s}^{-1}$, assuming the σ estimated above. It is unlikely that there is enough scatter in the scaling relations to accommodate $v_{\text{vir}} \approx 200 \text{ km s}^{-1}$ in VCC 128. Thus, its SMBH probably violates the proposed limit unless VCC 128 has been heavily stripped in the cluster environment. Curiously, however, VCC 128 would still satisfy the relation between M_{CMB} and B -band magnitude M_B (Wehner & Harris 2006; Ferrarese et al. 2006).

We have shown that the nucleus of VCC 128 is double, with the two components of equal magnitude and color. We propose that this can be explained by the presence of a disk surrounding a SMBH. Simple estimates of its mass all put it in the regime

$M_{\bullet} \sim 10^6 M_{\odot}$ or larger. If VCC 128 is on the fundamental plane, then these estimates put the SMBH at, or above, the M_{\bullet} - σ relation. However, the halo virial velocity would be smaller than the proposed limit for galaxies to be able to form SMBHs. Among the dwarf elliptical/spheroidal population of galaxies, this is only the second example of a system with evidence of a SMBH (Maccarone et al. 2005). Given the very interesting nature of this object, we suggest that further high-resolution imaging and spectroscopy of VCC 128 would be well worthwhile.

V. P. D. is supported by a Brooks Prize Fellowship at the University of Washington and receives partial support from NSF ITR grant PHY-0205413. S. D. R. acknowledges Postdoctoral Fellowship support from the Fund for Scientific Research, Flanders, Belgium (FWO). V. P. D. thanks the MPIA Heidelberg for hospitality during part of this project. We thank the anonymous referee for comments that helped to significantly improve this Letter.

REFERENCES

- Baes, M., Buyle, P., Hau, G. K. T., & Dejonghe, H. 2003, MNRAS, 341, L44
Bahcall, J. N., & Soneira, R. M. 1980, ApJS, 44, 73
Barth, A. J., Ho, L. C., Rutledge, R. E., & Sargent, W. L. W. 2004, ApJ, 607, 90
Binggeli, B., Sandage, A., & Tammann, G. A. 1985, AJ, 90, 1681
Bruzual, G., & Charlot, S. 2003, MNRAS, 344, 1000
Chabrier, G. 2003, PASP, 115, 763
Chandrasekhar, S. 1943, ApJ, 97, 255
Côté, P., et al. 2006, ApJS, 165, 57
De Rijcke, S., & Debattista, V. P. 2004, ApJ, 603, L25
de Rijcke, S., Michielsen, D., Dejonghe, H., Zeilinger, W. W., & Hau, G. K. T. 2005, A&A, 438, 491
Ferrarese, L. 2002, ApJ, 578, 90
Ferrarese, L., & Merritt, D. 2000, ApJ, 539, L9
Ferrarese, L., et al. 2006, ApJ, 644, L21
Filippenko, A. V., & Ho, L. C. 2003, ApJ, 588, L13
Fitzpatrick, E. L. 1999, PASP, 111, 63
Gebhardt, K., Rich, R. M., & Ho, L. C. 2002, ApJ, 578, L41
Gebhardt, K., et al. 2000, ApJ, 539, L13
———. 2001, AJ, 122, 2469
Geha, M., Guhathakurta, P., & van der Marel, R. P. 2002, AJ, 124, 3073
Greene, J. E., & Ho, L. C. 2004, ApJ, 610, 722
Jacobs, V., & Sellwood, J. A. 2001, ApJ, 555, L25
Jerjen, H., Binggeli, B., & Barazza, F. D. 2004, AJ, 127, 771
Kormendy, J., & Gebhardt, K. 2001, in AIP Conf. Proc. 586, 20th Texas Symp. on Relativistic Astrophysics, ed. J. C. Wheeler & H. Martel (Melville: AIP), 363
Kormendy, J., & Richstone, D. 1995, ARA&A, 33, 581
Kormendy, J., et al. 1997, ApJ, 482, L139
Lauer, T. R., et al. 1993, AJ, 106, 1436
———. 1996, ApJ, 471, L79
———. 2005, AJ, 129, 2138
Lotz, J. M., Miller, B. W., & Ferguson, H. C. 2004, ApJ, 613, 262
Maccarone, T. J., Fender, R. P., & Tzioumis, A. K. 2005, MNRAS, 356, L17
Merritt, D., & Ferrarese, L. 2001, ApJ, 547, 140
Merritt, D., Ferrarese, L., & Joseph, C. L. 2001, Science, 293, 1116
Peng, C. Y., Ho, L. C., Impey, C. D., & Rix, H.-W. 2002, AJ, 124, 266
Pickles, A. J. 1998, PASP, 110, 863
Salow, R. M., & Statler, T. S. 2001, ApJ, 551, L49
Sambhus, N., & Sridhar, S. 2002, A&A, 388, 766
Schlegel, D. J., Finkbeiner, D. P., & Davis, M. 1998, ApJ, 500, 525
Tonry, J. L., Dressler, A., Blakeslee, J. P., Ajhar, E. A., Fletcher, A. B., Luppino, G. A., Metzger, M. R., & Moore, C. B. 2001, ApJ, 546, 681
Tremaine, S. 1995, AJ, 110, 628
Tremaine, S., et al. 2002, ApJ, 574, 740
Valluri, M., Ferrarese, L., Merritt, D., & Joseph, C. L. 2005, ApJ, 628, 137
Wehner, E. H., & Harris, W. E. 2006, ApJ, 644, L17
Wyithe, J. S. B. 2006, MNRAS, 365, 1082